Structural refinement of 1/1 bcc approximants to quasicrystals: Bergman-type W(TiZrNi) and Mackay-type M(TiZrFe)

W. J. Kim, P. C. Gibbons, and K. F. Kelton
Department of Physics, Washington University, St. Louis, Missouri 63130

W. B. Yelon
University of Missouri, Research Reactor, Columbia, Missouri 65211
(Received 22 October 1997)

We report the structural refinement of large-unit-cell bcc crystalline phases found in Ti-Zr-Ni and Ti-Zr-Fe alloys, which are 1/1 rational approximants of icosahedral quasicrystals in the same alloys. The structure of the stable 1/1 phase W(TiZrNi), lattice constant $a_o = 14.317$ Å, determined by a Rietveld analysis of x-ray and neutron powder diffraction data, is closely related to that of the 1/1 phases R(AlLiCu) and Bergman(AlMgZn), containing Bergman-type icosahedral clusters of atoms. Despite the similar chemistry of the 1/1 phases in Ti-Zr-Ni and Ti-Zr-Fe alloys, the 1/1 phase M(TiZrFe) contains double-shell Mackay icosahedra, like those found in the 1/1 phase α(TiCrSiO). These results provide starting structures for six-dimensional refinements of the related quasicrystals. [S0163-1829(98)02729-5]

I. INTRODUCTION

Icosahedral quasicrystal (i phase) formation has been reported in Ti-(V, Cr, Mn, Fe, Co and Ni)-Si-O (Refs. 1–3) and Ti-Zr-(Fe, Co and Ni) alloys.[4–6] Complex crystalline phases called crystal approximants, which contain distorted icosahedra in their structures, have also been discovered in these alloys. These include the Ti_2Ni-type fcc phase, the $MgZn_2$-type C14 Laves phase, the $MgCu_2$-type fcc phase, and the 1/1 bcc rational approximants α(TiCrSiO),[3] M(TiZrFe),[4] and W(TiZrNi).[7] Structural similarities between crystal approximants and quasicrystals are revealed by the similar sequence of intense peaks in their diffraction patterns and a frequent common growth orientation. For the 1/1 approximant,[8] for example, $\langle 100\rangle_{1/1} \| 2\text{-fold}_{i\ \text{phase}}$ and $\langle 111\rangle_{1/1} \| 3\text{-fold}_{i\ \text{phase}}$.

Among these crystal approximants, the 1/1 rational approximants are important for understanding the structures of the quasicrystals because of their similar, yet solvable, local atomic structures. The atomic structures of the series of rational approximants can in principle be obtained by projecting from the six-dimensional (6D) hyperspace to the physical 3D space, with the orientation of the projection window taken as the ratio of successive numbers in the Fibonacci sequence, i.e., 1/1, 2/1, 3/2, 5/3,..., τ. The icosahedral phase is obtained when the projection window has slope τ (1.618...-the golden mean), which is the limit of the sequence of rational slopes. The simpler structure of the 1/1 approximant makes it a useful starting point in refinements of structures of icosahedral quasicrystal by lifting the 1/1 structure to 6D, reorientating the projection window, and reprojecting. Of course, the atomic surfaces must be refined along with the usual parameters.

The atomic structures of some 1/1 approximants are known, including α(AlMnSi),[9] the AlMgZn Bergman phase,[10] R(AlLiCu) (Ref. 11) and α(TiCrSiO).[3,12] Though these share a common structural unit, a double-shell icosahedron, small differences divide them into two distinct classes, Bergman[10] or Mackay[13] structures. The Mackay class divides further into two subclasses, for Ti or Al alloys. The fundamental cluster in the Bergman 1/1 approximant ($Im\bar{3}$), space group number 204, ($cI160$ or $cI162$) is a double-shell icosahedron with the face centers of the second shell occupied, forming a Pauling tricontahedron. Both the AlMgZn Bergman phase and the R(AlLiCu) phase belong to the Bergman class. The fundamental cluster in the Mackay 1/1 approximant ($Im\bar{3}$, space group number 204) is also a double-shell icosahedron, but with the edge centers of the second shell occupied rather than the face centers. The Al-Mackay-type 1/1 approximant α(AlMnSi), $cP138$, contains more vacant sites than the Ti-Mackay-type 1/1 α(TiCrSiO), $cI146$, likely reflecting the higher vacancy formation energy in titanium alloys. It was recently demonstrated that the i phases corresponding to these crystal approximants can be sorted into the same three classes (i.e., Bergman, Al-Mackay, and Ti-Mackay),[14] supporting the assumed structural similarity between the i phase and the 1/1 approximant. There, the ratio of measured quasilattice constant and atomic separation, estimated from the measured density of the icosahedral phases, was found to differ among the quasicrystal classes.

The formation of the i phase and the 1/1 approximant in Ti-Zr-Fe alloys was first reported by Kim and Kelton.[4] Unfortunately, the small amount of the 1/1 approximant found prevented the determination of its structure and hence made the classification of the corresponding quasicrystal difficult. A careful examination of the twofold selected area electron diffraction (SAD) patterns, however, shows that i(TiZrFe) contains strong arcs of diffuse scattering, similar to those observed for i(TiCrSiO). In contrast, diffraction patterns from i(TiZrNi) contain no such scattering artifacts, suggesting that despite their chemical similarity, i(TiZrFe) and i(TiZrNi) belong to different classes. In support of this, the classification method proposed by Kim, Gibbons, and

Kelton,[14] places i(TiZrFe) in the Ti-Mackay class with i(TiCrSiO) rather than with i(TiZrNi).

Here, that classification is confirmed, based on structural refinements of the 1/1 bcc approximants to the related quasicrystals in Ti-Zr-Ni and Ti-Zr-Fe alloys. The formation and plausible atomic structure of the 1/1 phase in Ti-Zr-Ni alloys, W(TiZrNi), was recently reported by Kim, Gibbons, and Kelton.[7] There, they indicate that the structure of the W phase should be similar to R(AlLiCu) or Bergman(AlMgZn). A Rietveld analysis of x-ray and neutron diffraction from W(TiZrNi) is presented here to confirm this. Structural refinements using x-ray-diffraction data from the 1/1 approximant in Ti-Zr-Fe alloys, M(TiZrFe), show that the Mackay cluster is the fundamental unit in the alloy, as it is in α(TiCrSiO).

II. EXPERIMENT

Ti-Zr-Ni and Ti-Zr-Fe alloys were prepared by arc melting in high purity Ar gas. A Ti-Zr-Ni ingot was placed in a graphite crucible, which was in turn placed inside a quartz tube along with the Ti-Zr alloy, to be used as an oxygen getter. The tube was then evacuated and sealed (10^{-5} -10^{-6} torr). To prevent oxygen contamination, the Ti-Zr getter was first heated to 1000 °C for 10 min by rf induction, while keeping the alloy ingot in the graphite crucible at room temperature. The tube containing the sample and the getter was then placed in a furnace and annealed at 610 °C for 64 h.

A Ti-Zr-Fe ingot was rf melted in a fused-silica tube that had been coated with zirconia to minimize silicon and oxygen contamination. The molten alloy was then ejected through a small hole in the bottom of the tube by pressurized Ar gas and quenched onto a rotating copper wheel with a typical surface velocity of 25 m/s. The resulting ribbons, identified as i(TiZrFe), were 2 mm wide, 20-45 μm thick and 3–15 cm long. Portions of these ribbons were heated in a Perkin-Elmer differential scanning calorimeter (DSC-7) to transform i(TiZrFe) to the 1/1 M(TiZrFe).

The phases present in the resulting samples were identified by powder x-ray diffraction using Cu $K\alpha$ radiation. Neutron powder diffraction data for the samples (800 mg of the W phase) were obtained at the Missouri University Research Reactor, located at the University of Missouri, Columbia, Missouri. The neutron wavelength was 1.7675 Å. A JEOL 2000FX transmission electron microscopy (TEM) equipped with a Noran energy dispersive x-ray spectrometer was used to characterize the sample microstructure and to obtain the phase compositions. Sample densities were determined by Archimedes weighing in toluene, using a computer-monitored Cahn microbalance. The structure of the W phase and the M phase were refined by the Rietveld method[15] using the general structure analysis system (GSAS).[16]

III. DIFFRACTION FROM W(TiZrNi) AND M(TiZrFe)

A typical x-ray-diffraction pattern from an as-cast ingot of Ti-Zr-Ni is shown in Fig. 1(a), which presents mostly C14 Laves hexagonal structure ($a=5.15$ Å and $c=8.27$ Å). The patterns for the 1/1 approximant, W(TiZrNi), and the icosahedral phase, i(TiZrNi), obtained by annealing at 610 °C and 570 °C, respectively, for 64 h are shown in Figs. 1(b) and 1(c). Based on the measured x-ray peaks, the lattice constant, a_o, of the W phase is 14.317 Å and the quasilattice constant a_q of i(TiZrNi) is 5.17 Å. TEM studies confirmed the identity of the i phase and the W phase in the two samples. Energy dispersive x-ray spectroscopy measurements in TEM give the composition of the W phase as $Ti_{44\pm2}Zr_{40\pm2}Ni_{16\pm1}$, identical to the composition of the as-cast ingots. The measured composition of the i phase was $Ti_{41.5\pm1}Zr_{41.5\pm1}Ni_{17\pm1}$.

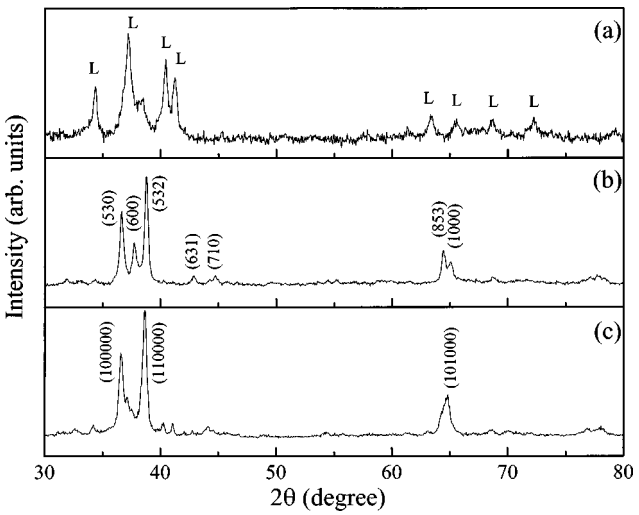

FIG. 1. X-ray-diffraction patterns of Ti-Zr-Ni alloys: (a) the as-cast sample; (b) after annealing at 610 °C and (c) after annealing at 570 °C for 64 h in Ti-Zr-Ni alloys.

A similarity in the primary x-ray peak positions for the W phase and the i phase is evident, suggesting that the local atomic configurations of the two phases are similar. This is even more evident in SAD patterns taken from the two phases. For example, the bright spot modulations of (530), (111), and (100) SAD patterns from the W phase [Figs. 2(a), 2(b), and 2(c), respectively] are very similar to the fivefold, threefold, and twofold patterns from the i phase [Figs. 2(d), 2(e), and 2(f)].

In contrast to i(TiZrNi), which is clearly a stable phase at 570 °C, i(TiZrFe) is metastable, transforming to more stable crystal phases upon heating. The exothermic crystallization peak (1.25 kJ/mol) of i(TiZrFe), measured upon heating at 10 °C/min in the DSC, is shown in Fig. 3(a). The x-ray-diffraction pattern of the as-quenched, predominantly i phase, ribbon is shown in Fig. 3(b). The ribbon contains some Ti_2Ni-type fcc phase, called here this T phase ($a_o=11.5$ Å). The quasilattice constant for this i phase is $a_q=4.85$ Å. Figure 3(c) shows the x-ray-diffraction pattern from the transformed sample. The transformation of the i phase leads to the formation of a phase mixture consisting of 1/1 bcc approximant, the M phase, $a_o=13.307$ Å, and a small amount of T phase. This indicates that the M phase is more stable than the i phase in these alloys. Whether this is also true of the T phase is uncertain since the formation of this phase is known to be stabilized by small amounts of oxygen, likely present during heating in the DSC.

The SAD patterns of the M phase along the (530), (111), and (100) zones are shown in Figs. 4(a), 4(b), and 4(c), re-

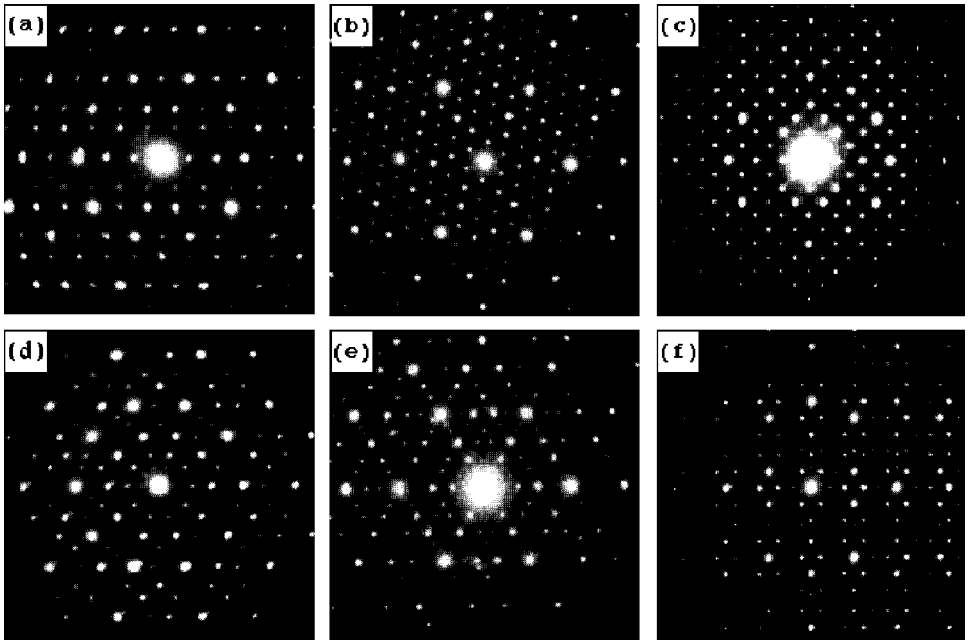

FIG. 2. Selected area diffraction patterns (SAD) of 1/1 *W* and *i* phases in Ti-Zr-Ni alloys: (a) (530), (b) (111), and (c) (100) zones of the *W* phase; (d) five, (e) three, and (f) twofold zones of the *i* phase.

spectively. The fivefold, threefold, and twofold zones for *i*(TiZrFe) are shown in Figs. 4(d), 4(e), and 4(f), respectively. The intense diffraction peaks from the *M* phase are, again, similar to those from the *i* phase, suggesting that the local atomic structures of these two phases are similar. The composition of the *M* phase, $Ti_{64}Zr_{11}Fe_{24}$, as measured by EDS is very close to that of the *i* phase, within 2 at.% of instrumental uncertainty.

For a true 1/1 approximant, the lattice constant $a_{1/1}$ can be determined from the quasilattice constant a_q of the related *i* phase using the following relation:[17]

$$a_{1/1}=a_q\left(4+\frac{8}{\sqrt{5}}\right)^{1/2}.$$

The measured values, 14.317 Å for *W*(TiZrNi) and 13.307 Å for *M*(TiZrFe), agree well with the values calculated from the measured quasilattice constants, 5.17 Å for *i*(TiZrNi) and 4.85 Å for *i*(TiZrFe), using this relation.

In both alloy systems, then, the x-ray and SAD patterns from the two 1/1 approximants [i.e., *W*(TiZrNi) and *M*(TiZrFe)] are similar to those diffraction patterns from the respective *i* phases. When comparing the diffraction patterns of the two 1/1 approximants, however, important differences can be identified. For example, the (620) peak from *M*(TiZrFe) is an intense peak [Fig. 3(c)], which is true of diffraction patterns from the 1/1 phase α(TiCrSiO), first reported and solved by Libbert *et al.*[3,12] In contrast, this peak is extremely weak in the pattern from *W*(TiZrNi). These differences, and others, in the diffraction patterns from the two phases indicate differences in their atomic structure, with that of the *M* phase most similar to that of α(TiCrSiO). Since the structure of α(TiCrSiO) is known to be constructed from Mackay icosahedra packed at the corner and body center of a cubic cell, this is likely the basic structure for the *M*(TiZrFe) as well, and gives some clues to the local structure of the TiZrFe *i* phase. The structure of *W*(TiZrNi), however, is different; the structure of *i*(TiZrNi) is likely also different from other Ti-based quasicrystals.

IV. STRUCTURAL REFINEMENT OF *W*(TiZrNi) AND *M*(TiZrFe)

A Rietveld analysis of the powder diffraction data from *W*(TiZrNi) and *M*(TiZrFe) was made to determine the atomic structures of these two phases. X-ray and neutron data were used for the refinement of the *W* phase, but only x-ray data were available for *M*(TiZrFe).

Three known atomic structures, α(AlMnSi), *R*(AlLiCu), and α(TiCrSiO), representatives of the known classes of 1/1 approximants, were used as starting structures for the refinement. The goodness of crystallographic fits are characterized by the residuals wR_p, R_p, and reduced χ^2, providing a standard measure of how well the calculated data match the observed data. In the GSAS these are defined as

$$R_p=\frac{\Sigma|I_o-I_c|}{\Sigma I_o},$$

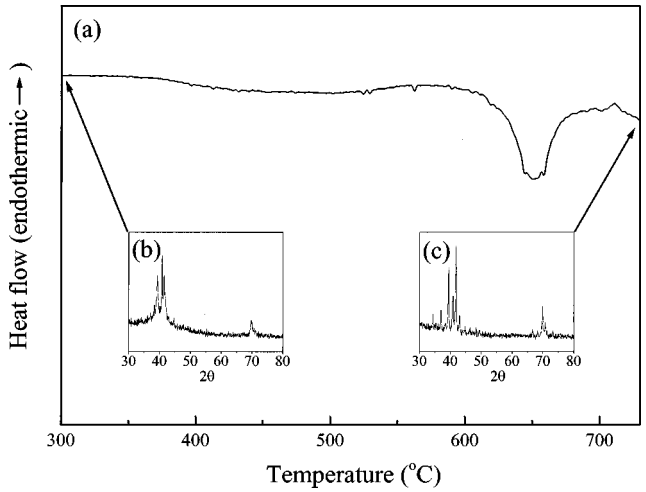

FIG. 3. (a) DSC trace of quenched ribbons showing an exothermic transformation from the *i* phase to the 1/1 approximant in Ti-Zr-Fe alloys. The x-ray-diffraction pattern from the as-quenched *i* phase (b) and after transformation to 1/1 *M*(TiZrFe) (c).

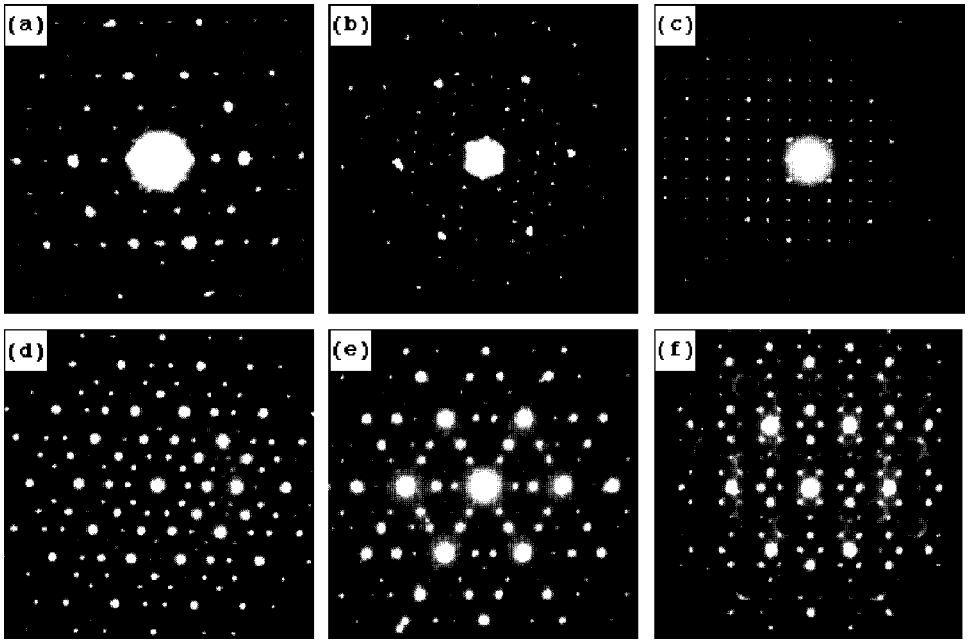

FIG. 4. Selected area diffraction patterns (SAD) of 1/1 *M* and *i* phases in Ti-Zr-Fe alloys: (a) (530), (b) (111), and (c) (100) zones of *M* phase; (d) five, (e) three, and (f) twofold zones of the *i* phase.

$$wR_p = \sqrt{\frac{M}{\Sigma w I_o^2}},$$

where

$$M = \sum w(I_o - I_c)^2.$$

The reduced χ^2 is given by

$$\chi^2 = \frac{M}{(N_{obs} - N_{var})}.$$

I_o and I_c are the observed and calculated integrated intensities, respectively, and w is a weighting factor. N_{obs} and N_{var} are the number of data points used in the fit and the number of fitting parameters, respectively. If χ^2 is less than 4, the fit has a crystallographic significance. The minimum values for the residuals depend on the statistical accuracy of the data to be fit and are determined by the GSAS program. The best fits were obtained assuming a *R*(AlLiCu)-type atomic structure for *W*(TiZrNi), and the α(TiCrSiO)-type atomic structure for *M*(TiZrFe), indicating the origin of the differences in the diffraction patterns from these two phases.

A. Fit to the *W*(TiZrNi) data

Of the three different atomic configurations discussed, only *R*(AlLiCu) gave reasonable results for *W*(TiZrNi); wR_p was 0.12 for neutron and 0.08 for x-ray-diffraction data and the combined reduced χ^2 was 2.85. The other two structures gave much larger errors, with the minimum reduced χ^2 near 8. Figure 5 demonstrates the good fit to the x-ray (a) and neutron (b) data. The crosses indicate the observed intensity as a function of scattering angle and the solid line is the calculated intensity using the atomic positions given in Table I. The differences between the observed and calculated diffraction intensities are shown in the bottom of Fig. 5. The composition of the refined structure for the *W* phase ($Ti_{43}Zr_{39.3}Ni_{17.8}$) agrees with the measured composition ($Ti_{44\pm2}Zr_{40\pm2}Ni_{16\pm1}$) to within 2 at.%.

B. Fit to the *M*(TiZrFe) data

The best fit to the diffraction data for the *M* phase was found by refining the α(TiCrSiO) starting structure. Here $wR_p \cong 0.55$ and the reduced χ^2 was 1.25. Again after refinement, the other starting structures gave much larger errors with a minimum reduced χ^2 of 9. A comparison between the measured data (crosses) and that calculated from the best refined structure (solid line) is shown in Fig. 6. The differences between the observed and calculated intensities are shown in the bottom of Fig. 6. The discrepancy can be reduced further by refining the two phases, i.e., the *M* phase

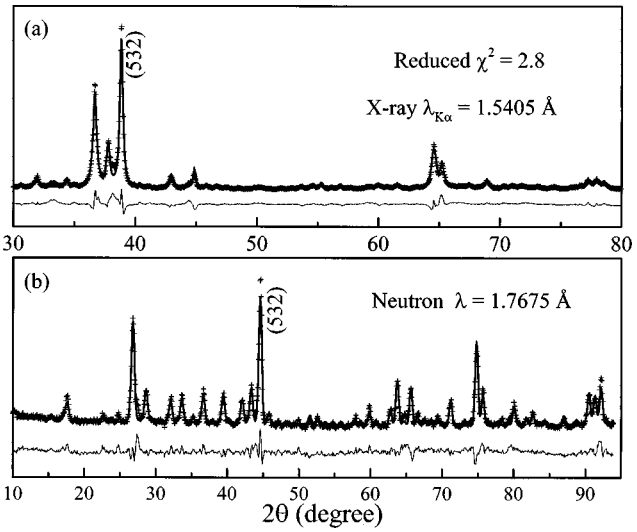

FIG. 5. The fit of the refined structure for 1/1 *W*(TiZrNi) to the x-ray-diffraction (a) and neutron-scattering data (b). The measured data are indicated by crosses (+); the fit is shown by the solid line. The differences between the fit and the data are given by the thin line at the bottom of each panel.

TABLE I. Refined structure of the 1/1 W(TiZrNi) phase showing the sites (Wycoff notation), unit-cell positions (the cell edge being 10^4 units long), site occupation, and distance from center d.

Atom positions and occupancies in W(TiZrNi)						
	$cI162$	Space group $Im\bar{3}$			$a_o = 14.317$ Å	
	Site	x	y	z	Occupancy	d (Å)
1	2(a)	0	0	0	Ni(0.8)	
2	24(g)	0	1049	1660	Ti(0.88), Zr(0.12)	2.811
3	16(f)	1894	1894	1894	Zr(1.00)	4.697
4	24(g)	0	3097	1130	Zr(1.00)	4.720
5	24(g)	0	1906	3115	Ni(0.87), Ti(0.13)	5.228
6	48(h)	1476	1883	4020	Ti(0.87), Ni(0.13)	6.698
7	12(e)	4075	0	5000	Zr(0.71), Ti(0.29)	7.280
8	12(e)	1965	0	5000	Zr(1.00)	7.691

and the T phase, together; the resulting structure of the M phase remains unchanged. The refined atomic positions are listed in Table II. Because the atomic refinement was done using only x-ray data, due to a limited amount of the sample, the occupation fraction for Fe and Ti on some sites could not be precisely determined. Also the oxygen sites occupied in α(TiCrSiO) could not be determined for M(TiZrFe), due to the small atomic x-ray form factor of oxygen. The calculated composition of the refined structure for the M phase ($Ti_{56.2}Zr_{18.4}Fe_{25.4}$) is richer in Zr and poorer in Ti than the measured composition ($Ti_{64\pm2}Zr_{11\pm2}Fe_{25\pm1}$). These differences might arise from possible silicon and oxygen contamination during sample preparation. The contributions of oxygen and silicon were ignored for the fit, because their concentrations are uncertain, and their x-ray form factors are much smaller than those of Ti, Fe, and Zr. Further, similar atomic scattering factors of Ti and Fe limit the distinguishability of these atoms in the structure. These differences in concentration should not change the structural type determined for this approximant.

V. DISCUSSION

As mentioned in the Introduction, the previously known 1/1 approximants are the α phase in AlMnSi alloys,[9] the AlMgZn Bergman phase,[10] the R phase in AlLiCu (Ref. 11), and the α phase in TiCrSiO.[3,12] Except for α(AlMnSi), all of these phases share the same space group symmetry, $Im\bar{3}$, space group number 204. In this section, the atomic structures for W(TiZrNi) and M(TiZrFe) will be discussed in comparison with these previously known 1/1 approximants.

A. W(TiZrNi)—A Bergman 1/1 approximant

The basic cluster for W(TiZrNi), $cI162$, is the Bergman-type cluster illustrated in Fig. 7. The cluster center is partially occupied by a Ni atom [no. 1-2(a) in the Wycoff notation of Table I]; this position is partially occupied in the Bergman phase of AlMgZn by Al, with nearly the same occupation probability. In contrast, this position is vacant in R(AlLiCu). The Ni atom is surrounded by 12 Ti/Zr atoms [no. 2-24(g) sites] making a nearly undistorted icosahedron. Titanium, the major component of W(TiZrNi), occupies 88% of these sites, which is exactly the fraction occupied by Al in R(AlLiCu). A larger, second-shell icosahedron is filled with 12 Ti/Ni atoms [no. 5-24(g) sites], having a high Ni occupancy of 87%. The face centers of the second shell are occupied by 20 Zr atoms [8 of no. 3-16(f) sites] and [12 of no. 4-24(g) sites], completing the dodecahedral Bergman cluster. Not shown in Fig. 7 is a truncated icosahedron formed by no. 6-48(h) sites, consisting of Ti atoms with an 87% occupancy, no. 7-12(e) sites, and a third-shell icosahedron formed by no. 8-12(e) sites, all lying outside the Bergman cluster.

In the W(TiZrNi) structure, Zr (the largest atom) occupies 71% of no. 7-12(e) sites while Ti (the smallest atom and the major component) occupies 29%. In contrast, these sites are entirely occupied by Mg (the largest atom), in Bergman(AlMgZn), and by Al (the smallest atom and the major component) in R(AlLiCu). In the R phase, the largest atom, Li, fills the no. 3-16(f), no. 4-24(g), and no. 8-12(e) sites (dodecahedron and third-shell icosahedron) with no remaining Li to occupy other sites. The number of these sites is insufficient, however, to contain all of the Mg in the Bergman phase, due to its higher concentration. The excess Mg occupies all of no. 7-12(e) sites. Because the concentration of the large atom, Zr, in the W phase is intermediate between the cases for the Bergman and R phase, some Zr occupy no. 7-12(e) sites after first filling the no. 3-16(f), no. 4-24(g), and no. 8-12(e) sites.

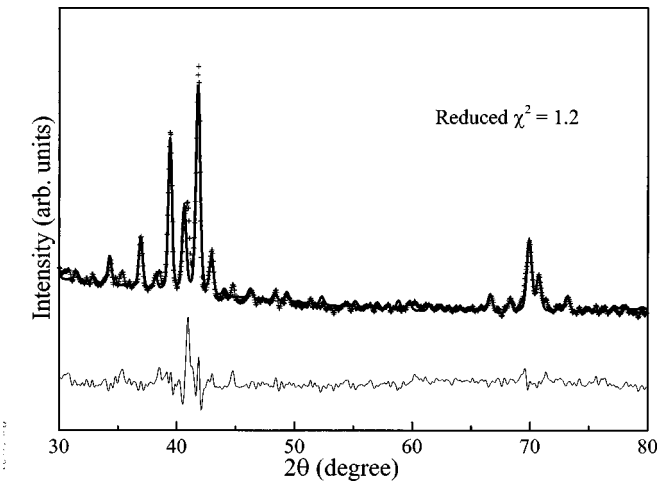

FIG. 6. The fit of the refined structure for 1/1 M(TiZrFe) to the x-ray-diffraction data. The measured data are indicated by crosses (+); the fit is shown by the solid line. The differences between the fit and the data are given by the thin line at the bottom of the panel.

TABLE II. Refined structure of the 1/1 M(TiZrFe) phase showing the sites (Wycoff notation), unit-cell positions (the cell edge being 10^4 units long), site occupation, and distance from center d.

Atom positions and occupancies in M(TiZrFe)						
	$cI146$	Space group $Im\bar{3}$			$a_o = 13.307$ Å	
	Site	x	y	z	Occupancy	d (Å)
1	2(a)	0	0	0	Zr(0.55), Fe(0.45)	
2	24(g)	0	1097	1819	Ti(0.62), Zr(0.38)	2.827
3	48(h)	1180	3065	1778	Ti(1.00)	4.970
4	12(d)	3821	0	0	Zr(1.00)	5.085
5	24(g)	0	2124	3226	Fe(1.00)	5.140
6	24(g)	0	3881	3481	Ti(0.80), Fe(0.20)	6.937
7	12(e)	0	3387	5000	Fe(0.61), Zr(0.39)	6.991

The distance from the center [no. 1-2(a)] to the vertex of the second-shell icosahedron [no. 5-24(g)] is 5.228 Å, less than two times the distance from the center to the vertex of the first-shell icosahedron, 2.811 Å. Assuming that the i phase and the 1/1 approximant can be constructed from identical rhombohedral units, the quasilattice constant a_q, should be comparable to the center-vertex distance for the second shell of the icosahedral cluster of the 1/1 approximant. This is approximately true for Bergman-type structures: $a_q = 5.04$ Å in i(AlLiCu) and $d = 5.05$ Å in R(AlLiCu); and $a_q = 5.17$ Å in i(TiZrNi) and $d = 5.228$ Å in W(TiZrNi), differing by just 1%.

B. M(TiZrFe)—A Ti-Mackay 1/1 approximant

The results of the structural refinement indicate that M(TiZrFe), $cI146$, is constructed from a face packing of two-shell Mackay icosahedra, similar to the structure for α(AlMnSi) and α(TiCrSiO). The α(AlMnSi) is primitive cubic ($pI138$) due to a large number of vacant sites. In contrast, the structures of M(TiZrFe) and α(TiCrSiO) are identical, having a true bcc phase and no vacant sites. This is likely due to the higher vacancy formation energy for Ti over Al.

The two-shell Mackay icosahedron of M(TiZrFe) is shown in Fig. 8. The center of the icosahedron [no. 1-2(a) in the Wycoff notation of Table II] is occupied by Fe and Zr atoms, similar to α(TiCrSiO) for which this site is occupied by the Cr and Si atoms. In M(TiZrFe) the center atom is surrounded by 12 Ti/Zr atoms on sites no. 2-24(g), forming the first-shell icosahedron. The 12 second-shell sites of the icosahedron [no. 5-24(g)] are occupied by Fe atoms. Twenty four Ti atoms [no. 3-48(h)] and six Zr atoms [no. 4-12(d)] sit on the edge centers of the second-shell icosahedron. Taken together, then, these 55 atoms form a two-shell Mackay icosahedron, identical to the fundamental cluster for α(TiCrSiO). Additionally, some vertices in the third shell of this icosahedron are occupied Fe/Zr [no. 7-12(e)]. Surprisingly, the distance from center [no. 1-2(a)] to the second-shell vertex of the icosahedron [no. 5-24(g)], 5.14 Å, is larger than the quasilattice constant of the related i phase, 4.85 Å. This same discrepancy was also observed for Ti-Cr-Si-O i phases and 1/1 approximants. The center to the second-shell vertex distance for the 1/1 approximant was 5.32 Å, while the quasilattice constant for the i phase was 4.78 Å. There this might be due to oxygen atoms sitting in octahedral sites located between the first- and second-shell icosahedra in α(TiCrSiO); it could arise for similar reasons in M(TiZrFe). While the procedures used to produce M(TiZrFe) provide opportunities for oxygen contamination, this cannot be confirmed without neutron-diffraction studies.

C. Contrast with other known 1/1 approximants

Table III summarizes the structural similarities and differences between W(TiZrNi), M(TiZrFe), and the four previously known 1/1 approximants. Three classes of 1/1 phases are evident. The Bergman(AlMgZn), R(AlLiCu), and

TABLE III. Comparison of the known 1/1 approximants.

Alloys	Ti-Zr-Ni	Ti-Zr-Fe	Ti-Cr-Si-O	Al-Li-Cu	Al-Mg-Zn	Al-Mn-Si
Space group	$Im\bar{3}$	$Im\bar{3}$	$Im\bar{3}$	$Im\bar{3}$	$Im\bar{3}$	$Pm\bar{3}$
Number of atoms in the unit cell	$cI162$	$cI146$	$cI146$	$cI160$	$cI162$	$cP138$
Occupation of cluster center	partial filled	filled	filled	empty	partial filled	empty
Center to 2nd shell vertex distance (Å)	5.23	5.14	5.32	5.05	5.05	4.61
Quasilattice constant of related i phase (Å)	5.17	4.85	4.78	5.04	5.04	4.60
Basic cluster	Bergman	Mackay	Mackay	Bergman	Bergman	Mackay
Class (Ref. 14)	Bergman	Ti-Mackay	Ti-Mackay	Bergman	Bergman	Al-Mackay

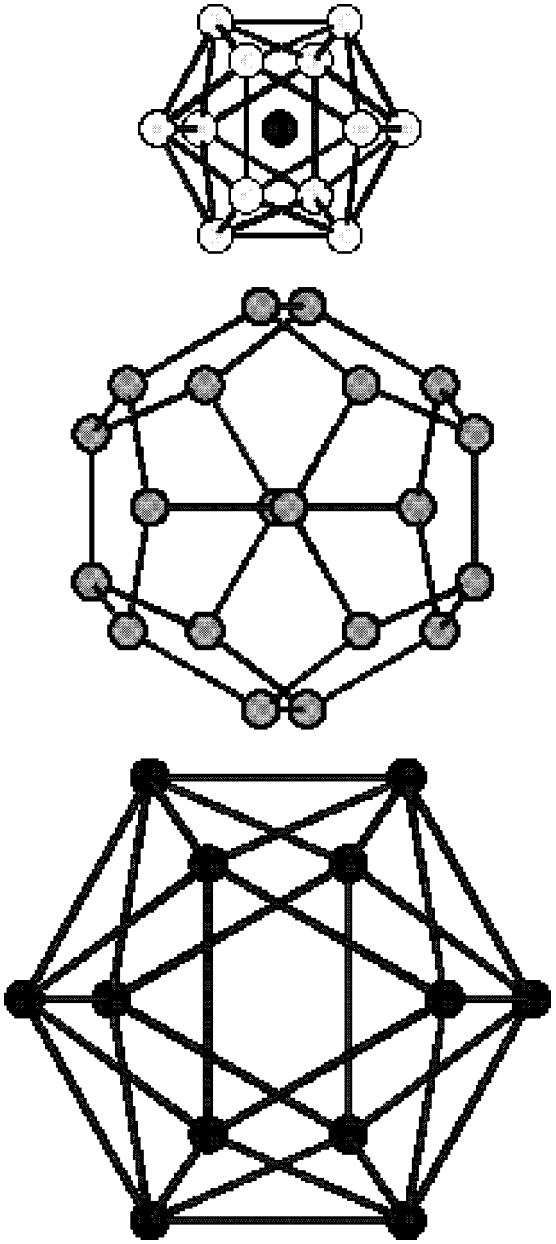

FIG. 7. The construction of the basic Bergman-type cluster for 1/1 W(TiZrNi); white (Ti dominant sites), gray (Zr atoms), and black (Ni dominant sites).

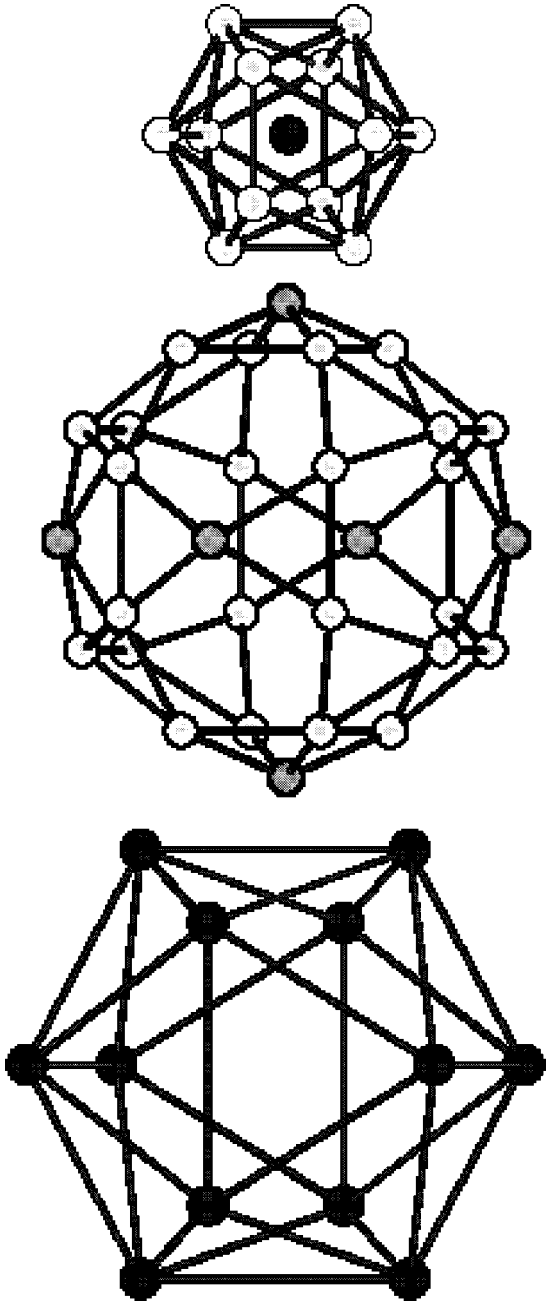

FIG. 8. The construction of the basic Mackay-type cluster for 1/1 M(TiZrFe); white (Ti dominant sites), gray (Zr atoms), and black (Fe dominant sites).

W(TiZrNi) 1/1 approximants are built around Pauling triacontahedra, two-shell Bergman-type icosahedra that contain atoms on the face centers of the second shell. Either 44 or 45 atoms reside in each cluster, depending on the occupation of the site at the center of the cluster, giving a total number of atoms in the unit cell of 160 or 162. The center to second-shell vertex distance is equal to the related i-phase quasilattice constant within 1%. The α(AlMnSi) 1/1 phase is in a second class. It contains 138 atoms in the unit cell and is constructed from two-shell Mackay icosahedra (called Al-Mackay icosahedra), having empty centers and atoms sitting on the edge centers in the second shells rather than on the face centers. The quasilattice constant 4.60 Å is also nearly equal to the center to second-shell vertex distance, 4.61 Å. The α(TiCrSiO) and M(TiZrFe) 1/1 approximants constitute a third class. A two-shell Mackay icosahedron (called a Ti-Mackay icosahedron) is the basic building block. In these, however, the central site is occupied giving a total of 55 atoms in the cluster. The total number of atoms in the unit cell is intermediate between the numbers in the other two classes, i.e., 146 atoms as opposed to 138 for the Al-Mackay class and 160 to 162 for the Bergman class. Also, unlike the first and second classes, the quasilattice constant for the i phase in Ti-Cr-Si-O and Ti-Zr-Fe alloys differs significantly from the center to second-shell vertex distance for the icosahedra in the approximant. The quasilattice constant ($a_q = 4.78$ Å) in i(TiCrSiO) is 10% smaller than the center-vertex distance ($d = 5.32$ Å) in α(TiCrSiO). It is 6% smaller in Ti-Zr-Fe alloys ($a_q = 4.85$ Å and $d = 5.14$ Å). The origin of this difference is uncertain. The high density of oxygen

atoms located in the octahedral sites between the first and second shells of the icosahedra in α(TiCrSiO) may move the second-shell atoms further from the center. The *i* phase in this alloy contains less oxygen,[2] perhaps giving a smaller distortion of the icosahedra believed to be fundamental to that structure and thus giving a smaller quasilattice constant. The amount of oxygen contained in the Ti-Zr-Fe *i* phases is as yet unknown, but a similar behavior might be expected.

Assuming that the local structures for the crystal approximants and the corresponding *i* phases are similar, three classes for the *i* phases might also be expected. This speculation was supported recently by a new *i*-phase classification technique,[14] based on the ratios of the measured quasilattice constants and the average atomic separations estimated from measured *i*-phase densities. By this method, *i*(TiZrFe) is classified with the Ti-Mackay class containing *i*(TiCrSiO), while all compositions of *i*(TiZrNi) are classified in the Bergman class, despite the similarity of the chemistry of two *i* phases. We have shown previously that the quasilattice constant of $i[Ti_{60}Zr_{15}(Fe_xNi_{25-x})]$ changes when the Fe/Ni ratio is varied, holding the Ti and Zr concentrations. It increases rapidly in samples with high Fe (from $x=25$ to 15), varying from 4.85 to 5.10 Å, but remains nearly constant at 5.10 Å in the high Ni samples (from $x=12$ to 0). The changes in the high Fe samples far exceed those expected simply from the size difference of the Fe and Ni atoms. These results may signal a transition in the local structure of the *i* phases, constructed from a mixture of the fundamental clusters of the two classes, the Ti-Mackay in *i*(TiZrFe) and the Bergman in *i*(TiZrNi). This interpretation is based on a comparison of the SAD patterns from this alloy series; they show that the intensity of the arcs of diffuse scattering change as the composition changes between that of a pure Mackay- and a pure Bergman-type icosahedral phase. The different structures identified here for the approximants, *W*(TiZrNi) and *M*(TiZrFe), support this previously proposed *i*-phase classification method and these conclusions about the local structures of the *i*-phase alloys.

VI. CONCLUSION

The results of a structural refinement of two new bcc 1/1 approximants in Ti/Zr based alloys, *W*(TiZrNi) and *M*(TiZrFe), are reported in this paper. The *W* phase was obtained by annealing as-cast Ti-Zr-Ni alloys at 610 °C for 64 h. The as-cast alloys initially contained only the C14 Laves phase and Ti-Zr solid solution phase. The *M* phase was obtained by heating rapidly quenched ribbons in a DSC; these initially contained primarily the *i* phase. Upon heating, an exothermic transformation 1.25 kJ/mol of the Ti-Zr-Fe *i* phase was observed, indicating that the *i* phase is metastable relative to the *M* phase.

The atomic structures of these phases were determined from a Rietveld analysis of powder x-ray and elastic neutron-scattering data for *W*(TiZrNi) but only x-ray data from *M*(TiZrFe). These refinements clearly demonstrate that these two 1/1 approximants are different; *W*(TiZrNi) is constructed from Bergman clusters while *M*(TiZrFe) is based on Mackay clusters. The *W* phase is isostructural with *R*(AlLiCu) and Bergman(AlMgZn), while the *M*(TiZrFe) appears to be isostructural with α(TiCrSiO). The possible presence of oxygen in the *M*(TiZrFe), known to be important for the formation of the α(TiCrSiO), could not be confirmed, however, without neutron-scattering data. The measured quasilattice constants and center to second-shell vertex distances are approximately equal for all Bergman 1/1 approximants [Bergman(AlMgZn), *R*(AlLiCu), and *W*(TiZrNi)] and for Al-Mackay [α(AlMnSi)]. They differ by as much as 10%, however, for the Ti-Mackay approximants [α(TiCrSiO) and *M*(TiZrFe)].

ACKNOWLEDGMENTS

The authors thank J. L. Libbert for useful discussions and H. H. Luo for taking the neutron data. This work was partially supported by the NSF under Grant Nos. DMR-92-03572 and DMR-97-05202.

[1] K. F. Kelton, P. C. Gibbons, and P. N. Sabes, Phys. Rev. B **38**, 7810 (1988).
[2] K. F. Kelton, Int. Mater. Rev. **38**, 105 (1993).
[3] J. L. Libbert, K. F. Kelton, A. I. Goldman, and W. B. Yelon, Phys. Rev. B **49**, 11 675 (1994).
[4] W. J. Kim and K. F. Kelton, Philos. Mag. A **72**, 1397 (1995).
[5] W. J. Kim and K. F. Kelton, Philos. Mag. Lett. **74**, 439 (1996).
[6] S. A. Sibirtsev, V. N. Chebotnikov, V. V. Molokonov, and Y. K. Kovneristyi, Pis'ma Zh. Eksp. Teor. Fiz. **47**, 644 (1988) [JETP Lett. **47**, 744 (1988).].
[7] W. J. Kim, P. C. Gibbons, and K. F. Kelton, Philos. Mag. Lett. **76**, 199 (1997).
[8] X. Zhang and K. F. Kelton, Philos. Mag. Lett. **63**, 39 (1991).
[9] M. Cooper and K. Robinson, Acta Crystallogr. **20**, 614 (1966).
[10] G. Bergman, J. T. Waugh, and L. Pauling, Acta Crystallogr. **10**, 157 (1957).
[11] M. Audier, J. Pannetier, M. Lebranc, C. Janot, J. Lang, and B. Dubost, Physica B **153**, 136 (1988).
[12] J. L. Libbert and K. F. Kelton, Philos. Mag. Lett. **71**, 153 (1995).
[13] A. L. Mackay, Physica A **114**, 609 (1982).
[14] W. J. Kim, P. C. Gibbons, and K. F. Kelton, Philos. Mag. A (to be published).
[15] H. M. Rietveld, J. Appl. Crystallogr. **2**, 65 (1969).
[16] A. C. Larson and R. B. Von Dreele, Los Alamos National Lab. Report No. LAUR 86-748, 1994 (unpublished).
[17] V. Elser and C. L. Henley, Phys. Rev. Lett. **55**, 2883 (1985).